Effects of organised media on the excited-state proton transfer in 2-(2′-pyridyl)benzimidazole

Madhab C. Rath, Dipak K. Palit and Tulsi Mukherjee*†
Chemistry Division, Bhabha Atomic Research Centre Mumbai 400 085, India

Absorption and fluorescence characteristics of 2-(2′-pyridyl)benzimidazole (2-PBI) are studied in the presence of α- and β-cyclodextrins (CD) in aqueous solution at two different pHs. Steady-state and time-resolved fluorescence measurements are used for the investigation of the effect of organised media on the excited-state proton transfer reaction in 2-PBI. Semi-empirical CI calculation for the geometry of the molecule reveals that the 2-PBI molecule may be involved in host–guest complex formation with α-CD and β-CD in different configurations. NMR measurements corroborate this, providing information about the orientation of the 2-PBI molecule inside the cavity of the CDs. No complex formation was evident in γ-CD owing to its larger cavity dimension compared to the size of the 2-PBI molecule.

Derivatives of benzimidazole are known to exhibit interesting photochemical and photophysical properties,[1–5] *e.g.* excited-state proton transfer (ESPT) for proton transfer lasers.[6–8] In particular, the protonated pyridyl derivatives of benzimidazole undergo photoinduced PT reactions in the excited singlet state[9,10] owing to different acid–base properties.[11] These processes are extremely fast, of the order of picoseconds. This type of study can provide information about the structure, configuration and energy states of the molecules in the excited state and their suitability as laser dyes[12,13] and photostabilisers for polymers.[14]

Photophysical properties of pyridylbenzimidazoles in various organic solvents have been studied by Kondo[15] and Brown *et al.*[16] Kondo[15] observed that the fluorescence of 2-(2′-pyridyl)benzimidazole (2-PBI) was considerably quenched in alcoholic solvents compared to other solvents and also compared to other pyridyl isomers in alcohols. This anomalous behaviour of 2-PBI molecule in alcohols has been attributed to hydrogen atom transfer from the imidazole ring to the pyridyl nitrogen atom, facilitated by alcohols probably forming a bridge-type hydrogen-bonded complex. ESPT reactions of 2-PBI molecules in aqueous solution have been studied by Prieto *et al.*[9] Four different protonated/deprotonated species of 2-PBI in the ground state have been identified, depending on the acidity of the medium. In acid media (pH *ca.* 3), the monocation (C), which is protonated at the benzimidazole nitrogen atom (N) exhibits dual fluorescence, one of the bands (at *ca.* 466 nm) having a large Stokes' shift with respect to the normal emission band (at *ca.* 380 nm) has been attributed to the formation of an excited species (T*), due to photoinduced PT from the benzimidazole nitrogen atom to the pyridyl nitrogen atom (Scheme 1).

Here, we report the effect of change in the microenvironments around the 2-PBI molecule in aqueous solution on its ESPT properties, studied by steady-state and time-resolved fluorescence and ^{1}H NMR. CDs, known to form inclusion complexes with molecules of compatible size, *i.e.* with a good match between the host and the guest molecules,[17,18] may affect the microenvironment around the probe molecules by hydrophobic interactions.[19] Such interactions have been used to investigate the ESPT properties of different compounds in aqueous solutions.[20,21] Three types of CDs, differing in the number of glucose rings α-CD (six rings), β-CD (seven rings) and γ-CD (eight rings)], having central cavities of different fixed sizes, are supposed to influence the microenvironment differently by accommodating different parts of the probe molecule inside their cavity.

Experimental

Materials

Pure 2-PBI was kindly supplied by Prof. K. C. Dash, Utkal University, Bhubaneswar. CDs were obtained from Fluka. All solutions were freshly prepared using water from Barnstead's nanopure water filtering assembly, having specific conductivity < 0.1 μS cm^{-1}. GR grade $HClO_4$ and NaOH were used to adjust the pH.

Apparatus

A Shimadzu UV–VIS-160A spectrophotometer was used for the ground-state absorption measurements. Steady-state fluorescence measurements were performed on a Hitachi model F-4010 spectrofluorimeter. A time-correlated single-photon counting spectrometer (Edinburgh Instruments, model 199) was used for the fluorescence lifetime measurements. A hydrogen-filled coaxial flashlamp with *ca.* 1 ns time duration (FWHM) was used as the excitation source. The fluorescence decay curves were analysed by a deconvolution procedure using a proper instrument response function. An Orion ionalyser 901 coupled with a glass electrode was used for the measurement of pH. ^{1}H NMR measurements were carried out in D_2O solutions on a Bruker Avance DPX-300 NMR spectrometer employing a solvent suppression technique. All measurements were made at room temperature (298 K).

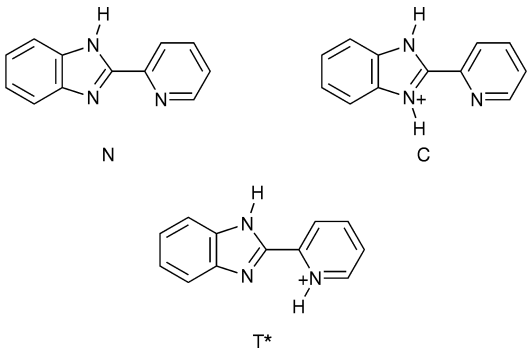

N C T*

Scheme 1

† E-mail: mukherji@magnum.barc.ernet.in

Preparation of samples

Aqueous solutions of 2-PBI (*ca.* 1×10^{-5} mol dm^{-3}) were prepared by sonicating a mixture of 2-PBI powder and nanopure water. Aqueous solutions of CDs (*ca.* 3×10^{-2} mol dm^{-3} α-CD and *ca.* 1.5×10^{-2} mol dm^{-3} β-CD) were prepared by taking the required amounts of the CDs by weight and dissolving them in the stock solution of 2-PBI. Aliquots were diluted with the stock solution of 2-PBI to get solutions with the same concentrations of 2PBI but different concentrations of α-CD and β-CD. The pH of the solutions was adjusted by adding $HClO_4$ or NaOH, allowing for the pK_a values of the CDs and their stability in aqueous solution.[22] The pK_a values of α-, β- and γ-CDs are 12.33, 12.20 and 12.08, respectively.[22] They undergo acid hydrolysis at pH < 3.5, and are unstable at higher temperature. It has been found that they are fairly stable between pH 3.5 and 11 and at temperatures lower than 60 °C.[22] Our experiments were carried out under these conditions. The lowest pH used for the ESPT study was 3.8 as the ground-state pK_a of the monocation to neutral 2-PBI equilibrium is 4.41. Quinine sulfate in 0.5 mol dm^{-3} H_2SO_4 ($\phi = 0.55$)[23] was taken as the standard for determination of fluorescence quantum yields (ϕ).

Results and Discussion

Fluorescence characteristics of 2-PBI in three non-aqueous solvents: methanol, acetonitrile and cyclohexane, reveal emission maxima at 361 nm ($\phi = 0.06$), 370 nm ($\phi = 0.75$) and 349 nm ($\phi = 0.75$), respectively, with fluorescence lifetimes of 0.2 ns (53%) and 1.5 ns (47%) in methanol, 1.10 ns in acetonitrile and 1.16 ns in cyclohexane. The emission maxima and the fluorescence lifetime values determined in our laboratory are in perfect agreement with those reported by Brown *et al.*[16] The very low quantum yield (0.06) in methanol compared to those in cyclohexane (0.75) and acetonitrile (0.75) can be explained by strong intermolecular hydrogen bonding in methanol with one of the solvent alcohol molecules involving both the benzimidazolyl and pyridyl nitrogen atoms, as shown in Scheme 2. In addition, the biexponential nature of the fluorescence decay in methanol shows the existence of two different hydrogen-bonded structures in equilibrium (**I** and **II**) in the excited singlet state. The longer-lived component can possibly be associated with the normal form, **I** and the shorter-lived one with the proton transfer form, **II**, as will become evident in the course of this study.

Fig. 1 (inset) shows the ground-state UV–VIS absorption spectra of 2-PBI in the absence and the presence of 2.2×10^{-2} mol dm^{-3} α-CD at pH 7. A spectral shift of *ca.* 5 nm to longer wavelength suggests a preferential binding of 2-PBI within the α-CD cavity. However, the change in the absorption spectra is too small to allow estimation of the binding constant using a Benesi–Hildebrand plot.[24] Similar changes were observed at pH 3.8 with α-CD, but no detectable changes were observed in the absorption spectra of 2-PBI in the presence of β-CD at either pH.

The fluorescence spectra showed considerable changes upon addition of α-CD and β-CD. However, addition of γ-CD did not produce any change in the photophysical behaviour of

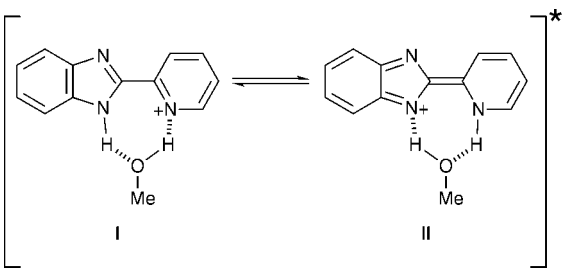

Scheme 2

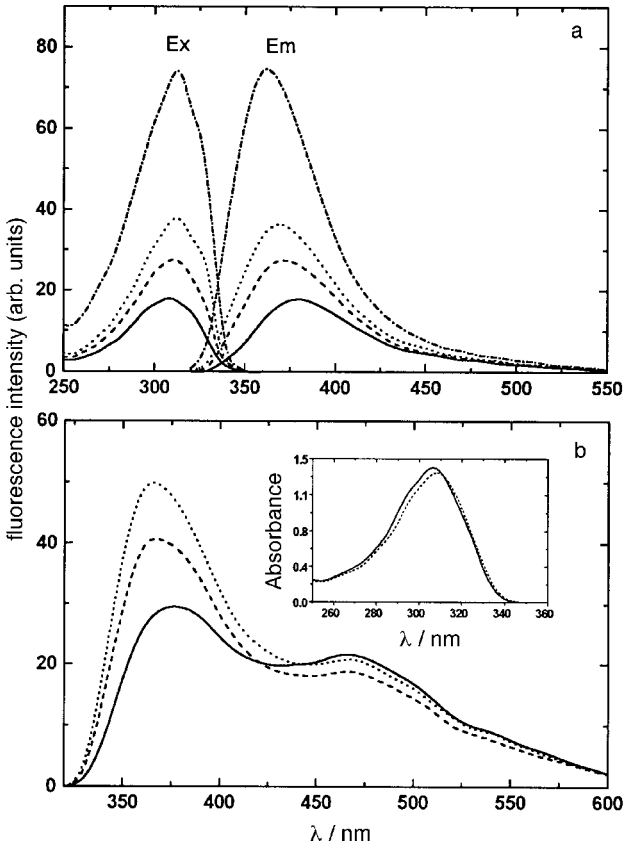

Fig. 1 (a) Corrected excitation and fluorescence spectra of 2-PBI at pH 7 in the presence of (———) 0.0, (– – – –) 0.24, (· · · · · ·) 0.5 and (· – · – ·) 2.2×10^{-2} mol dm^{-3}. (b) Corrected fluorescence spectra of 2-PBI at pH 3.8 the presence of: (———) 0.0, (– – – –) 0.8 and (· · · · · ·) 2.2×10^{-2} mol dm^{-3}. Inset: absorption spectra of 2-PBI in aqueous solution at pH 7, (———) in the absence and (– – – –) in the presence of 2.2×10^{-2} mol dm^{-3} α-CD.

2-PBI molecules, probably owing to the larger cavity size compared to the size of the 2-PBI molecule. Fig. 1 shows the corrected fluorescence spectra of 2-PBI in aqueous solution in the absence and presence of different concentrations of α-CD at pH 7 and 3.8, respectively. The photophysical parameters for 2-PBI determined from the steady-state and time-resolved fluorescence studies are given in Table 1. At pH 7, where only the neutral form (N) of 2-PBI exists in solution, the fluorescence spectra showed a blue shift of *ca.* 17 nm in the emission maximum, from 380 nm in the absence of α-CD, to 363 nm in its presence. The fluorescence quantum yield (ϕ) is increased from 0.05 in aqueous solution to 0.14 in the presence of 2.2×10^{-2} mol dm^{-3} α-CD. A *ca.* three-fold increase in the fluorescence quantum yield suggests the absence of bridge type hydrogen-bonded complex formation (Scheme 2) in the presence of α-CD, because a proton-transposition-like mechanism, operated *via* the intermolecularly hydrogen-bonded bridge-type complex, has been found to be responsible for fluorescence quenching of 2-PBI in alcoholic and aqueous solutions. A red shift of *ca.* 5 nm has also been observed for the fluorescence excitation maximum at this pH. These observations confirm the interaction of 2-PBI molecule with α-CD.

At pH 3.8, where the singly protonated cation form (C) of the molecule exists in solution, the emission maximum at 380 nm showed a blue shift of *ca.* 12 nm to 368 nm in the presence of 2.2×10^{-2} mol dm^{-3} α-CD. The fluorescence quantum yield also increased marginally compared to that in pure aqueous solution (Table 1). Unlike the case of 2-PBI alone, where there is a more than three-fold increase in the quantum yield from pH 7 to pH 3.8, there is a less than two-fold increase in the quantum yield in the presence of α-CD over

Table 1 Photophysical parameters of 2-PBI in aqueous solution

pH	chemical system	K/ dm^3 mol^{-1}	ϕ_{tot}	λ_{em}/nm	species emitting	τ/ns	remarks
3.8	2-PBI	—	0.17	380	C*	0.84	single exp. decay at 380 nm
				466	T*	1.80	rise time of 0.86 ns at 500 nm
3.8	2-PBI + αCD	100	0.23	368	C*	0.9(0.6)	double exp. decay
					(C–α-CD)*	2.6(0.4)	at 370 nm
				466	T*	2.1	rise time of 0.9 ns at 500 nm
3.8	2-PBI + βCD	60	0.16	375	C*	0.9(0.93)	double exp. decay
					(C–βCD)*	2.3(0.07)	at 370 nm
				466	T*	—	non-exp. at 500 nm
7	2-PBI		0.05	380	N*	0.06(0.48)	double exp. decay
						1.10(0.52)	at 370 nm
7	2-PBI + αCD	36	0.14	363	N*	1.2(0.42)	double exp. decay
					(N–αCD)*	2.8(0.48)	at 370 nm
7	2-PBI + *β*CD	—[a]	0.05	374	N*	0.28(0.67)	double exp. decay
					(N–*β*CD)*	1.35(0.33)	at 370 nm

[a] K value could not be determined accurately since there was very little change in the fluorescence characteristics.

this pH range. However, the major change in the spectral characteristics observed at pH 3.8 is the reduction of the peak intensity at 466 nm relative to that at 368 nm. The former has been assigned to the species T*, formed after the ESPT reaction.[9] No shift of the 466 nm fluorescence peak was observed in the presence of α-CD. The large increase in the quantum yield of 2-PBI alone in aqueous solution on change in pH from 7 to 3.8 has been attributed mainly to the ESPT phenomenon. In the presence of α-CD the decrease in intensity at 466 nm relative to that at 368 nm suggests that there could be a restricted environment created around the molecule, owing to formation of an inclusion complex which does not favour the ESPT reaction (see later).

In Fig. 2, the corrected fluorescence spectra of 2-PBI in the presence of β-CD has been compared with those in its absence at pH 7 and 3.8, respectively. In these cases also, the emission maximum at 380 nm shows a blue shift at both pHs (6 nm and 5 nm at pH 7 and 3.8, respectively), but to a lesser extent than in the presence of α-CD and without any shift of the 466 nm peak. While the fluorescence quantum yield in the presence of β-CD decreased marginally at pH 3.8, no significant change was observed at pH 7 (Table 1). It is evident that the fluorescence characteristics of 2-PBI have been affected to different extents by the two CDs.

We have studied the effect of pH on the emission characteristics of 2-PBI molecule in the presence of the highest concentrations of CDs used in our experiments. Fig. 3 shows the variation in the peak intensities of the two fluorescence bands of 2-PBI with pH in the presence of CDs. The trends of all the curves, except that representing the near-UV band of the 2-PBI–α-CD system, are similar to that of 2-PBI alone in aqueous solution.[9] The peak intensity of the near-UV band in the 2-PBI–α-CD system remains more or less constant for pH 6.5–9.5, but decreases gradually from pH 6.5–3.8, which is in reverse order to that in 2-PBI alone or in the 2-PBI–β-CD systems. The decrease in intensity of this band above pH 10 is due to the formation of the deprotonated species A, and pK_{NA} (*ca.* 12) was not affected by the presence of CDs. To rationalise the decrease in intensity of the 368 nm peak in the pH range 6.5–3.8 in the presence of α-CD, individual contributions of the fluorescence of N* or C* and T* in the total fluorescence spectra have been obtained by fitting the individual bands with the gaussian line spectra function, such that the sum of the individual spectra reproduce the experimental fluorescence spectra. One such representative fitted spectra for 2-PBI alone at pH 3.8 is shown in Fig. 4. The individual relative quantum yields of C* (ϕ_C) and T* (ϕ_T) fluorescence are presented in Table 2. T does not exist in the ground state, the relative quantum yield of T*, which is supposed to be formed by ESPT from C* or N* [eqn. (I)], has been evaluated by calculating the ratios of the individual integrated areas corresponding to T* and N* or C*. Table 2 shows that the relative quantum yields of C* and T* at pH 7 are not significantly different in the presence of β-CD as from those of 2-PBI alone in aqueous solution. However, in the presence of α-CD, ϕ_C

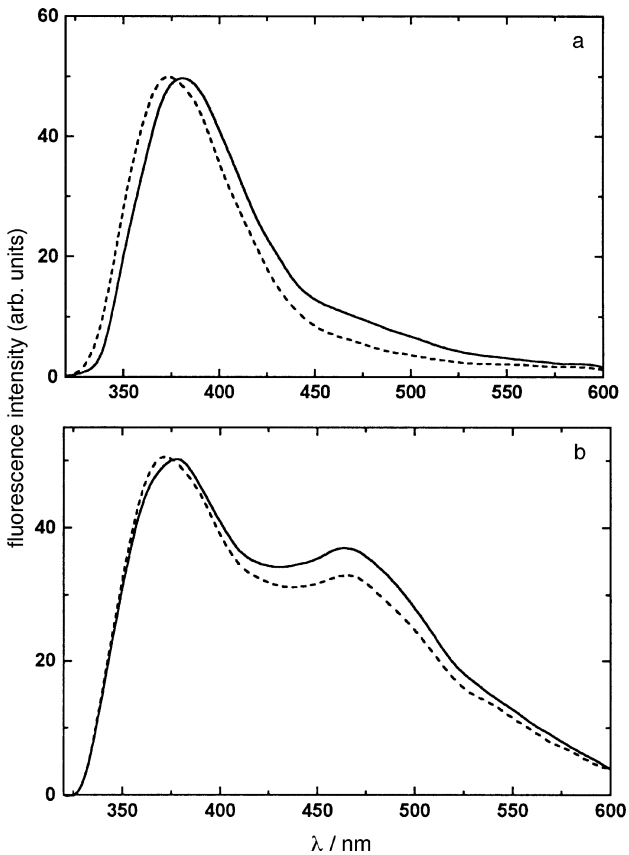

Fig. 2 (a) Corrected fluorescence spectra of 2-PBI at pH 7 in the presence of β-CD: (——) 0.0 and (– – – –) 1.45 × 10^{-2} mol dm^{-3}. (b) Corrected fluorescence spectra of 2-PBI at pH 3.8 in the presence of β-CD: (——) 0.0 and (– – – –) 1.45 × 10^{-2} mol dm^{-3}.

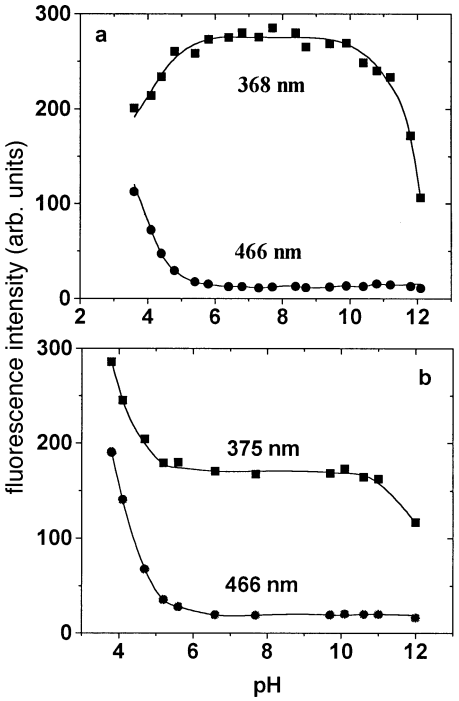

Fig. 3 Change in fluorescence intensity of 2-PBI with pH in the presence of (a) 2.4×10^{-2} mol dm^{-3} α-CD and (b) 1.3×10^{-2} mol dm^{-3} β-CD

increases *ca.* three-fold, whereas ϕ_T reduces considerably. This result indicates that, in the 2-PBI–α-CD complex, the 2-PBI molecule has been well shielded from the water molecules in the medium, thus preventing reaction, as suggested by Prieto *et al.*[9]

$$N^* + H_2O \rightleftharpoons T^* + OH^- \quad (I)$$

In the presence of β-CD the yield of T* *via* reaction (I) is reduced by half. At pH 3.8 also, the ESPT yield was affected considerably in the presence of α-CD but the yield of T* was not affected.

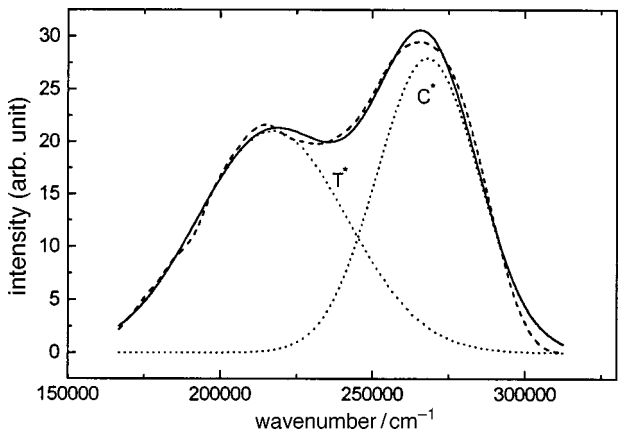

Fig. 4 Corrected fluorescence spectra of 2-PBI molecule at pH 3.8 together with the gaussian fit for the individual bands: (———) experimental curve, (– – – –) fitted summed curve and (·····) individual curves

Table 2 Fluorescence quantum yields of 2-PBI in the presence of α-CD and β-CD at different pH

system	pH	ϕ_{total}	ϕ_N	ϕ_C	ϕ_T(relative) = $(\phi_{total} - \phi_N)/\phi_N$
2-PBI	7	0.05	0.045		0.11
2-PBI	3.8	0.17		0.09	0.90
2-PBI–α-CD	7	0.14	0.14		0.00
2-PBI–α-CD	3.8	0.23		0.13	0.77
2-PBI–β-CD	7	0.05	0.048		0.04
2-PBI–β-CD	3.8	0.16		0.08	0.90

These changes in the fluorescence characteristics of 2-PBI in the presence of CDs definitely indicate the formation of inclusion complexes. To characterise these complexes it is essential to determine the association constants and also to find out in which conformation the 2-PBI molecule has been introduced into the CD cavity. Determination of these parameters should provide information about the change in microenvironment of the probe molecule on formation of the host–guest complex. Quantitative data on the stoichiometric ratio and association constants of the inclusion complexes of 2-PBI with CDs may be calculated from their fluorescence characteristics using the Benesi–Hildebrand equation.[24] Assuming 1 : 1 complex formation,

$$2\text{-PBI} + \text{CD} \rightleftharpoons 2\text{-PBI–CD} \quad (II)$$

$$K = \frac{[2\text{-PBI–CD}]}{[2\text{-PBI}][\text{CD}]} \quad (1)$$

where, [2-PBI–CD], [2-PBI] and [CD] are the equilibrium concentrations of the complex, 2-PBI and CD, respectively. The concentration of CD being very large compared to that of the complex formed in the mixture, we assume, $[CD]_o \approx [CD]$, where the subscript 'o' indicates the initial concentration. Rearrangement of eqn. (1), replacing the various concentrations by the fluorescence intensity parameters gives:

$$\frac{1}{I - I_o} = \frac{1}{I_1 - I_o} + \frac{1}{K[CD]_o(I_1 - I_o)} \quad (2)$$

Hence, in the case of 1 : 1 complex formation, a plot of $1/(I - I_o)$ *vs.* $1/[CD]_o$ should give a straight line and from its slope and intercept, the K value can be calculated. For a 2 : 1 complex the corresponding equation may be written as:

$$\frac{1}{I - I_o} = \frac{1}{I_1 - I_o} + \frac{1}{K[CD]_o^2(I_1 - I_o)} \quad (3)$$

Here, a plot of $1/(I - I_o)$ *vs.* $1/[CD]_o^2$ should give a straight line and from its slope and intercept the K value for a 2 : 1 complex can be calculated.

Benesi–Hildebrand plots following eqn. (2) for 2-PBI in the presence of α-CD and β-CD at pH 3.8 gave straight line plots. The association constants (K) are calculated from the linear fit of the experimental points and are listed in Table 1. A 1 : 1 association between 2-PBI and the CDs is clearly indicated at both pHs. No linear plot was obtained by plotting $1/(I - I_o)$ *vs.* $1/[CD]_o^2$ according to eqn. (3) in either case and, hence, the possibility of formation of a 2 : 1 complex is ruled out. Note that the K value is lower at pH 7 than at pH 3.8 in the case of the complex with α-CD. However, owing to the very small difference in fluorescence characteristics between 2-PBI and the 2-PBI–β-CD inclusion complex, particularly at pH 7, the errors involved in the K values determined are much higher than those for α-CD. However, it is certain that the interaction between 2-PBI and α-CD is stronger than that between 2-PBI and β-CD.

A knowledge of the orientation of the 2-PBI molecule inside the CD cavities is necessary to characterise the photophysical properties of the inclusion complex quantitatively. For this, it is essential to have a knowledge of the molecular dimensions of the probe molecule, as well as the CD cavities. The reported internal cavity diameters (average) of α-CD and β-CD are 4.9 and 6.2 Å, respectively, but the cavity depth of both the CDs is 7.8 Å.[25] We have obtained the molecular dimensions of the 2-PBI molecule from a semi-empirical (CI) calculation, the result of which, for the ground-state of the neutral form of the molecule, has been presented in Table 3 and the molecular dimensions (Scheme 3) were calculated with the help of the parameters listed in this table.

Table 3 Theoretically calculated geometrical parameters for the optimised ground state of 2-PBI

bond length[a,b]				bond angle[a,c]			
N1—H	0.986	C4—C5	1.384	N1—C2—N3	110.0	N3—C2—C2′	125.1
C4—H	1.100	C5—C6	1.409	C2—N3—C9	105.4	C2—C2′—C3′	119.0
C5—H	1.100	C6—C7	1.384	N3—C9—C8	109.6	C3′—C2′—N1′	122.7
C6—H	1.100	C7—C8	1.405	C9—C8—N1	109.6	N1′—C2′—C2	118.3
C7—H	1.100	C8—C9	1.454	C8—N1—C2	105.4	C2′—N1′—C6′	119.3
C3′—H	1.100	C8—N	1.393	C8—C9—C4	119.3	C2′—C3′—C4′	118.5
C4′—H	1.100	C2—C2′	1.477	C9—C4—C5	118.3	C3′—C4′—C5′	119.3
C5′—H	1.097	C2′—C3′	1.412	C9—C8—C7	121.2	C4′—C5′—C6′	123.0
C6′—H	1.105	C3′—C4′	1.398	C8—C7—C6	117.5	C5′—C6′—N1′	118.5
N1—C2	1.414	C4′—C5′	1.392	C7—C6—C5	119.3	H—C5′—C4′	121.5
C2—N3	1.356	C5′—C6′	1.409	C6—C5—C4	121.2		
N3—C9	1.403	C6′—N1′	1.391	H—N1—C2	125.0		
C9—C4	1.405	N1′—C2	1.362	N1—C2—C2′	125.0		

[a] The numbers indicate the position of the corresponding atoms in the molecule (Scheme 3); [b] Bond lengths are in Å. [c] Bond angles are in degrees.

The results of these calculations reveal that the neutral form (N) of the molecule, in its most stable configuration in the ground state, is nearly flat, with the aromatic rings of both the pyridyl and the benzimidazolyl parts lying in the same plane. The distance between the H atoms at 4′ and 6′, which represents the physical width of the pyridyl part of the 2-PBI molecule, is *ca.* 4.6 Å, whereas the width of the benzimidazole part (*i.e.* distance between the H atoms at 4 and 7) is 5.1 Å. It is evident that, in the case of the 2-PBI–α-CD complex, only the pyridyl part of the 2-PBI molecule can be accommodated inside the α-CD cavity. The width of the benzimidazole part being larger than the cavity diameter of α-CD, this part must be outside the cavity. As the distance between the H atom at 5′ and the carbon atoms at 8 and 9 is 7.5 Å, for the 2-PBI–α-CD complex, the benzimidazolic nitrogen atoms are expected to be near the wider face of the α-CD molecule, providing extra stability to the host–guest complex *via* hydrogen-bond formation with the secondary hydroxy groups of the CD molecule. On the other hand, for the 2-PBI–β-CD complex, the pyridyl part of the probe molecule becomes a loose fit and the benzimidazole part should fit well into the cavity. These theoretical calculations give reasonable preliminary information about the complexation.

The actual description of the orientation of the 2-PBI molecule inside the cavity of CDs has been obtained from NMR measurements. 300 MHz ^{1}H NMR spectra of saturated solutions of 2-PBI taken in D_2O at neutral pH in the absence and presence of the highest concentrations of the CDs (both α- and β-CD) are shown in Fig. 5, which also shows the assignments of the NMR peaks and the hydrogen atoms that they are due to. There is a downfield tendency of the NMR peaks corresponding to the pyridyl protons (P_3, P_4 and P_6) in the presence of α-CD when compared to the corresponding peaks obtained in the absence of α-CD. However, owing to the weak nature of the hydrogen-bonding interaction between the benzimidazolic nitrogen atoms and the secondary hydroxy groups of α-CD, the shift in the NMR peaks is very small (0.08, 0.03 0.05 and 0 for P_3, P_4, P_6 and P_5, respectively) without any appreciable change in the peak shape or the splitting patterns. The interaction involving the benzimidazolic nitrogen atoms is also evident from the broadening and splitting pattern of the benzimidazolic hydrogen atoms, B_3, B_4, B_5 and B_6. These observations support our prediction from the theoretical calculations that, owing to the size factor, the pyridyl part of the 2-PBI molecule together with the benzimidazolic nitrogen atoms should be included in the α-CD cavity.

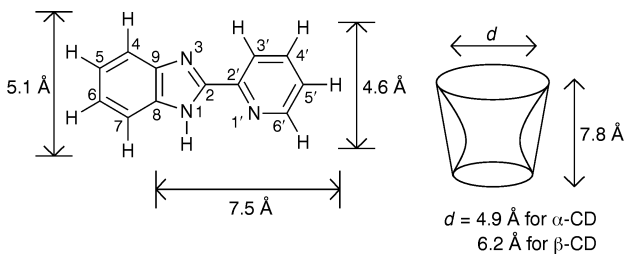

Scheme 3

However, formation of an inclusion complex in β-CD is not so conclusively evident from the NMR measurement. Although the broadening and the change in the splitting pattern of the peaks due to B_4, B_5 and B_3, B_6 indicate interaction between the benzimidazolic nitrogen atoms of 2-PBI and the secondary hydroxy groups of β-CD, no shift of these peaks has been observed due to the presence of β-CD. On the other hand, the pyridylic protons, except P_3 which is close to the benzimidazolic protons and has shown a downfield shift of 0.04 ppm, have not been affected by complexation with β-CD. It is evident that, in the 2-PBI–β-CD inclusion complex, the benzimidazole part resides inside the β-CD cavity, although the complexation in this case should be very weak.

In the 2-PBI–α-CD complex, the pyridyl nitrogen atom is shielded by the cavity in a hydrophobic environment. Therefore, the one-step concerted mechanism[26] of the ESPT from the benzimidazole nitrogen atom to the pyridyl nitrogen atom *via* a water molecule (Scheme 2 with H in place of Me), as suggested by Prieto *et al.*,[9] is not possible. So the ESPT process is observed to be reduced in this solution *via* the reduction in the fluorescence intensity at 466 nm peak. However, in the case of the 2-PBI–*β*-CD inclusion complex, the pyridyl part being in aqueous solution, the ESPT reaction is not much affected in the presence of β-CD because nothing prevents the pyridyl nitrogen atom from being protonated by another agent residing in the solution.

Time-resolved fluorescence measurements are consistent with the presence of two species and provide more information about the orientation of the probe molecule inside the cavities of the CDs. Fluorescence lifetimes (τ) have been determined for 2-PBI in aqueous solution in the presence and absence of different concentrations of CDs at two different pHs, 3.8 and 7, and at two different wavelengths, 375 nm and 500 nm (Table 1). The lifetimes of 2-PBI in aqueous solution without CDs are in good agreement with those reported by Prieto *et al.* At pH 7, where only the neutral molecule (N) exists in the solution, the fluorescence decay is double-exponential. The shorter component (60 ps) of the two lifetime values reported for the dual-exponential decays must be regarded as an upper-limit value, as it is beyond the limits of resolution of the instrument. However, there is no doubt that the decay follows a dual- rather than a single-exponential process. The dual-exponential nature of the fluorescence decay of 2-PBI in aqueous solution can be explained by the concerted hydrogen atom transfer from the benzimidazolic nitrogen atom to the pyridyl nitrogen atom, mediated by a water molecule (Scheme 2 with Me replaced by H). As evident from

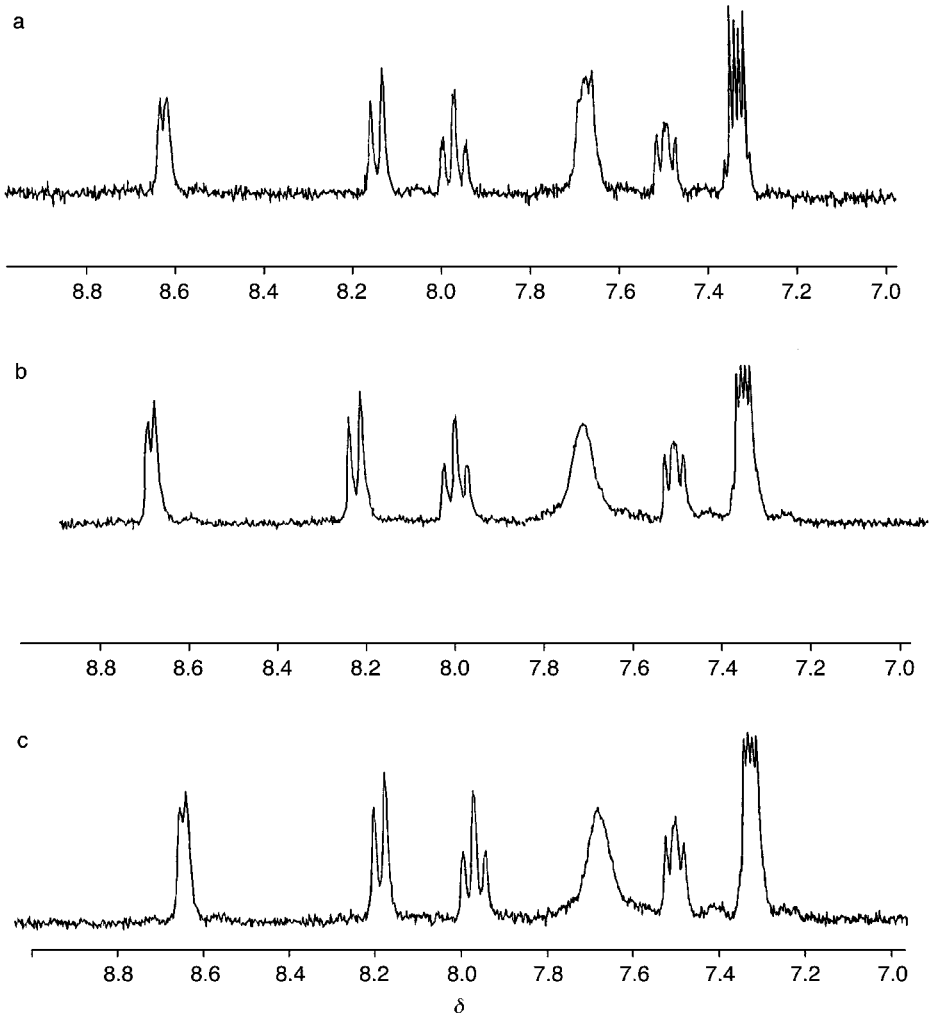

Fig. 5 300 MHz ^{1}H NMR spectra of (a) 2-PBI, (b) 2-PBI in the presence of α-CD and (c) 2-PBI in the presence of β-CD, in D_2O

the fluorescence spectra, some percentage of the proton transfer form T* is formed, even at pH 7. However, it is very small in all three cases. The relative fluorescence quantum yields, $\phi_T = (\phi_{Total} - \phi_N)/\phi_N$ from the ESPT form are listed in Table 2.

At pH 3.8, while the fluorescence decay of 2-PBI measured at 380 nm is single exponential ($\tau = 0.84$ ns) and can be assigned as due to the monocation, C, the decay measured at 500 nm has a growing component having a rise time of 0.86 ns and a decaying component having a lifetime of 1.8 ns. Prieto *et al.*[9] have assigned the latter to the proton-transferred form, T*, which has been formed from the excited state of the monocation, C*.

In the presence of α-CD at pH 7, the fluorescence decay is double exponential with lifetimes of 1.2 and 2.8 ns. The first component possibly corresponds to the free N molecules and the latter to the N–α-CD inclusion complex. However, in this case, the shorter component of N ($\tau = 60$ ps) is not detected. The fluorescence decay of 2-PBI at pH 3.8 in the presence of α-CD measured at 375 nm in the emission band of the monocation (C*) is double exponential in nature (Fig. 6, top). The shorter (0.9 ns) component is clearly assignable to the free monocation of 2-PBI in the bulk solution, whereas the longer-lived (2.6 ns) component is due to the inclusion complex. The fluorescence decay measured in the emission band of the proton-transferred form (T*) at 500 nm in the presence of α-CD at pH 3.8 also fits to a decay trace (Fig. 6, bottom) with a rise time of 0.9 ns and decay time of 2.1 ns. Thus, it is evident that, at pH 3.8, only the free 2-PBI molecules residing in the bulk aqueous phase undergo ESPT to form the T*

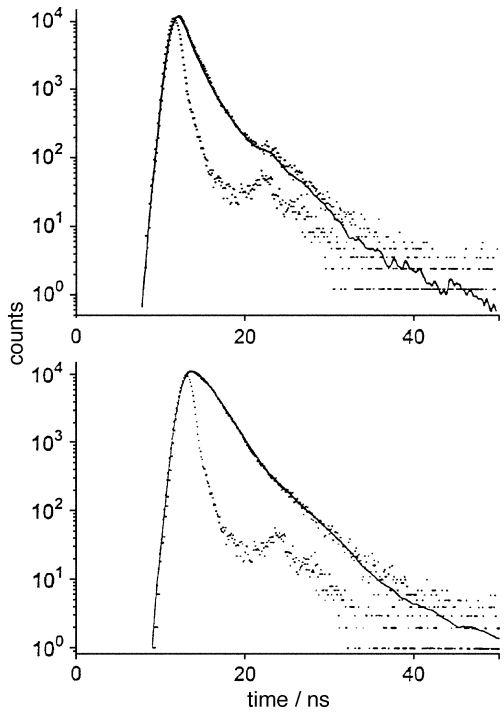

Fig. 6 Fluorescence decay curves of 2-PBI in the presence of *ca.* 2.0×10^{-2} mol dm^{-3} α-CD. Top: pH 3.8, $\lambda_{ex} = 310$ nm, $\lambda_{em} = 375$ nm; bottom: pH 3.8, $\lambda_{ex} = 310$ nm, $\lambda_{em} = 500$ nm.

state. However the inclusion complex, due to its restricted geometry, cannot undergo ESPT.

In the presence of β-CD at pH 7, the fluorescence decay of 2-PBI is double exponential with lifetimes of 0.28 and 135 ns, which can be compared to those obtained in methanol. This observation further confirms that, at this pH, the inclusion complex 2-PBI–β-CD is either very weak or absent in the solution, whereas the 2-PBI molecules see an environment which is equivalent to that in methanolic solution. At pH 3.8, where the complexation with β-CD is stronger than at pH 7, as is evident from the K values (Table 1), the fluorescence decay measured at 370 nm is also double exponential with decay components of 0.9 and 2.3 ns, which are very similar to those obtained with α-CD. Hence the shorter and longer components can be assigned to free 2-PBI and the 2-PBI–β-CD inclusion complex, respectively. However, the fluorescence decay measured at 500 nm is non-exponential and no meaningful lifetimes could be recovered for the fluorescence decay. This non-exponential behaviour of the fluorescence decay of T* indicates that not only free 2-PBI molecules but also the 2-PBI–β-CD inclusion complex undergo ESPT and the T* formed in these two cases have different lifetimes.

The authors thank Dr D. K. Maity, Chemistry Division, BARC for his help with the CI calculation and Profs. A. K. Singh and I. I. T. Mumbai, and Mr V. Sudarsan, Chemistry Division, BARC, for the NMR spectra. The authors also thank Prof. K. C. Dash, Utkal University, Bhubaneswar for providing 2-PBI in a pure form and the referees for some useful suggestions.

References

1 C. A. S. Potter and R. G. Brown, *Chem. Phys. Lett*., 1988, **153**, 7.
2 H. K. Sinha and S. K. Dogra, *Bull. Chem. Soc. Jpn*., 1989, **62**, 2668.
3 H. K. Sinha and S. K. Dogra, *Spectrochim. Acta, Part A*, 1989, **45**, 1289.
4 K. Das, N. Sarkar, A. K. Ghosh, D. Majumdar, D. N. Nath and K. Bhattacharyyaa, *J. Phys. Chem*., 1994, **98**, 9126.
5 A. Douhal, F. Amat-Guerri, A. U. Acuna and K. Yoshihara, *Chem. Phys. Lett*., 1994, **217**, 619.
6 A. Douhal, F. Amat-Guerri, M. P. Lillo and A. U. Acuna, *J. Photochem. Photobiol. A*, 1994, **78**, 127.
7 R. Duchowicz, M. Ferrer, F. Amat-Guerri, R. Sastre and A. U. Acuna, *Opt. Commun*., 1994, **104**, 336.
8 M. L. Ferrer, A. U. Acuna, F. Amat-Guerri, A. Costela, J. M. Figuera, F. Florido and R. Sastre, *Appl. Opt*., 1994, **33**, 2266.
9 F. R. Prieto, M. Mosquera and M. Novo, *J. Phys. Chem*., 1990, **94**, 8536.
10 M. Novo, M. Mosquera and F. R. Prieto, *J. Phys. Chem*., 1995, **99**, 14726.
11 J. F. Ireland and P. A. H. Wyatt, *Adv. Phys. Org. Chem*., 1978, **12**, 131.
12 D. A. Parthenopoulos and M. Kasha, *Chem. Phys. Lett*., 1988, **146**, 77.
13 A. U. Acuna, A. Costela and J. M. Munoz, *J. Phys. Chem*., 1986, **90**, 2807.
14 W. Klopffer, *Adv. Photochem*., 1977, **10**, 311.
15 M. Kondo, *Bull. Chem. Soc. Jpn*., 1978, **51**, 3027.
16 R. G. Brown, N. Entwistle, J. D. Hepworth, K. W. Hodgson and B. May, *J. Phys. Chem*., 1982, **86**, 2418.
17 J. M. Schutte, T. Ndou, A. Munoz de la Pena, K. L. Greene, C. K. Williamson and I. M. Warner, *J. Phys. Chem*., 1991, **95**, 4897.
18 A. Munoz de la Pena, T. Ndou, J. B. Zung and I. M. Warner, *J. Phys. Chem*., 1991, **95**, 3330.
19 T. Yorozu, M. Hoshimo, M. Imamura and H. Shizuka, *J. Phys. Chem*., 1982, **86**, 4422.
20 E. L. Roberts, P. T. Chou, A. Alexander, R. A. Agbaria and I. M. Warner, *J. Phys. Chem*., 1995, **99**, 5431.
21 J. E. Hansen, E. Pines and G. R. Fleming, *J. Phys. Chem*., 1992, **96**, 6904.
22 S. Li and W. C. Purdy, *Chem. Rev*., 1992, **92**, 1457.
23 W. H. Melhuish, *J. Phys. Chem*., 1961, **65**, 229.
24 H. A. Benesi and J. H. Hildebrand, *J. Am. Chem. Soc*., 1949, **71**, 2703.
25 V. Ramamurthy, *Tetrahedron*, 1986, **42**, 5753.
26 W. P. Jencks, *Acc. Chem. Res*., 1976, **9**, 425.

Paper 8/00369F; *Received* 13*th January*, 1998